On the kinetic mechanism of dimethylarginine dimethylaminohydrolase (DDAH) †

*Corey M. Johnson [a,b] and Walter Fast [a]**

[a] Division of Chemical Biology and Medicinal Chemistry, College of Pharmacy, University of Texas, Austin, Texas, 78712, USA

[b] Department of Chemistry and Biochemistry, Howard College of Arts and Sciences, Samford University, Birmingham, Alabama, 35229, USA

†Submitted as part of the joint virtual special issue honoring Richard Silverman

* corresponding author; walt.fast@austin.utexas.edu; ORCID: 0000-0001-7567-2213

Keywords: rapid quench-flow, methylarginine, covalent intermediate, global fitting, dimethylarginine

Abstract

Dimethylarginine dimethylaminohydrolase (DDAH, EC 3.5.3.18) catalyzes the hydrolysis of asymmetric N^{ω},N^{ω}-dimethyl-L-arginine (ADMA), an endogenous inhibitor of human nitric oxide synthases. The active-site cysteine residue has been proposed to serve as the catalytic nucleophile, forming an *S*-alkylthiourea reaction intermediate, and serving as a target for covalent inhibitors. Inhibition can lead to ADMA accumulation and downstream inhibition of nitric oxide production. Prior studies have provided experimental evidence for formation of this covalent adduct but have not characterized it kinetically. Here, rapid quench-flow is used with ADMA and the DDAH from *Pseudomonas aeruginosa* to determine the rate constants for formation (k_2 = 17 $\pm$ 2 s^{-1}) and decay (k_3 = 1.5 $\pm$ 0.1 s^{-1}) of the covalent *S*-alkylthiourea adduct. A minimal kinetic mechanism for DDAH is proposed that supports the kinetic competence of this species as a covalent reaction intermediate and assigns the rate-limiting step in substrate turnover as hydrolysis of this intermediate. This work helps elucidate the different reactivities of *S*-alkylthiourea intermediates found among the mechanistically diverse pentein superfamily of guanidine-modifying enzymes and provides information useful for inhibitor development.

.

1. Introduction

The production of nitric oxide (•NO) by •NO synthases is involved in numerous healthy cell signaling pathways and in pathophysiologies.[1-3] Overproduction of •NO is detrimental in various disease states including sepsis, some cancers, and neurodegeneration, driving the need to develop inhibitors of •NO synthases as potential therapeutics.[3-5] Among other labs, Silverman and coworkers have studied the mechanism of •NO synthases, developed novel types of inhibitors, determined methods to achieve isoform selective inhibition, and improved the drug-like qualities of •NO synthase inhibitors.[6-10] As a complement to these efforts, an alternative strategy to modulate •NO biosynthesis is to use an indirect approach by altering the concentration of the two endogenous •NO synthase inhibitors N^{ω}-monomethyl-L-arginine (L-NMMA) and asymmetric N^{ω},N^{ω}-dimethyl-L-arginine (ADMA), which are released by proteolysis of posttranslationally-methylated proteins.[11, 12] ADMA is a reversible inhibitor of •NO synthases, and L-NMMA is a time-dependent irreversible inhibitor that can be classified as a mechanism-based enzyme inactivator.[13-16] Endogenous methylarginine concentrations are regulated by their catabolic enzyme dimethylarginine dimethylaminohydrolase (DDAH).[17] This enzyme has been targeted by inhibitors to raise concentrations of the endogenous methylarginines, leading to downstream •NO synthase inhibition. Because DDAH expression patterns differ from •NO synthases, inhibition can occur in a tissue-selective manner that can be advantageous in some disease states.[11, 18-20]

The catalytic mechanism of DDAH is of interest to facilitate inhibitor design and to better elucidate transformations catalyzed by other guanidine-modifying enzymes in the pentein superfamily.[21] DDAH has a proposed mechanism that uses covalent catalysis to hydrolyze the guanidine of L-NMMA and ADMA to produce the urea-containing amino acid L-citrulline and (di)methylamine products (Figure 1).[22] A catalytic Cys nucleophile is proposed to form a transient *S*-alkylthiourea intermediate during the reaction, and this adduct has been trapped and characterized using alternative substrates, mutated DDAH, X-ray crystallography and mass

spectrometry.[23, 24] However, the rate constants for formation and decay of this proposed intermediate have not been determined. It is possible that the observed covalent adduct may accumulate due to an off-pathway artifact caused by the various perturbations used to trap the adduct and may not represent a true reaction intermediate. Here, we address this issue by using transient kinetics to establish a minimal kinetic mechanism for turnover of the endogenous ADMA substrate by wild type DDAH, primarily to determine if the *S*-alkylthiourea covalent adduct is a catalytically competent reaction intermediate.

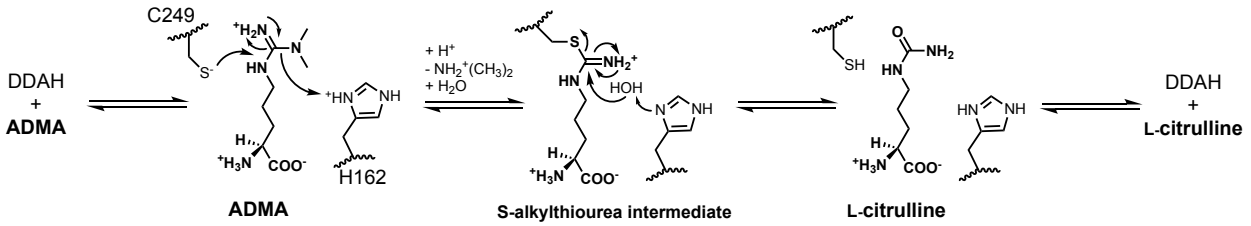

Figure 1. Proposed chemical mechanism of DDAH-catalyzed ADMA hydrolysis. Residue numbering corresponds to *Pseudomonas aeruginosa* DDAH.

2. Results and discussion

To trap and quantify the proposed covalent intermediate in DDAH turnover of ADMA, we initially used a strategy applied to a related enzyme in which an acidic quenching solution was used to stabilize the same S-alkylthiourea group adducted to the active-site Cys of arginine deiminase.[25, 26] For our studies, we used the DDAH from *Pseudomonas aeruginosa*. There have been more mechanistic studies completed using this ortholog and it is considered to be a good model of human DDAH1, which typically has lower purification yields.[22-24, 27, 28] Inspired by publications from Silverman and coworkers,[29, 30] among others, that used acid or base treatments of inactivated enzymes to help determine the identity of covalent adducts, we reasoned that the trapped *S*-alkylthiourea adduct with DDAH would be susceptible to hydrolysis by treatment with excess base, and result in release of additional L-citrulline product that could be used to help quantify adduct formation and decay rates. Therefore, we also used this approach. Finally, we

used denaturing mass spectrometry of the enzyme, acid quenched at various timepoints to detect the covalent adduct formation and decay over time. By using the chemical (in)stability of the covalent *S*-alkylthiourea adduct to trap and quantify different sets of reaction species using a rapid quench-flow instrument, we could then use global fitting to fit all data points simultaneously and construct a minimal kinetic mechanism for DDAH turnover of ADMA.

Our initial hypothesis was that the minimal kinetic mechanism of DDAH can be described by the scheme found in Figure 2, which uses the following designations: E, enzyme (DDAH); S, substrate (ADMA); ES, the noncovalent enzyme-substrate complex (DDAH:ADMA); E-I, the covalent *S*-alkylthiourea intermediate; P, the first product (dimethylamine); EQ, the noncovalent enzyme-product complex (DDAH:L-citrulline); and Q, the second product (L-citrulline). The various reaction species trapped using differing chemical treatments are described below and summarized in Figure 2.

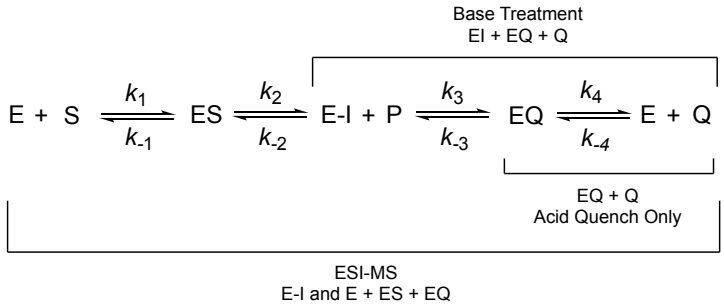

Figure 2. Hypothesized kinetic mechanism of DDAH and a summary of the species trapped using different conditions.

2.1 Acid quench

We used an acid quench to stop the reaction of ADMA and DDAH at various timepoints after mixing. The quenched solutions were assayed using an established method that derivatizes all available urea groups (e.g. the L-citrulline product) in the reaction mixture to produce a colored species that was then quantified by comparison to a standard curve prepared using L-citrulline standards.[31, 32] Due to the acidic conditions used in the quenching reaction, this procedure enables detection and quantification of the sum of two species, the released L-citrulline product

(Q) and L-citrulline bound to the enzyme through non-covalent interactions (EQ) that is released upon denaturation of the protein by acid and heat during the assay. Prequenched samples did not show any appreciable production of [Q + EQ] species (not shown). Conditions were chosen where ADMA concentrations exceeded that of the DDAH concentration to allow multiple turnovers. Using these procedures, we observed a brief lag period followed by increasing concentrations of [Q+EQ] (Figure 3a). These observations are consistent with the expected product formation catalyzed by DDAH. Global fitting is described below.

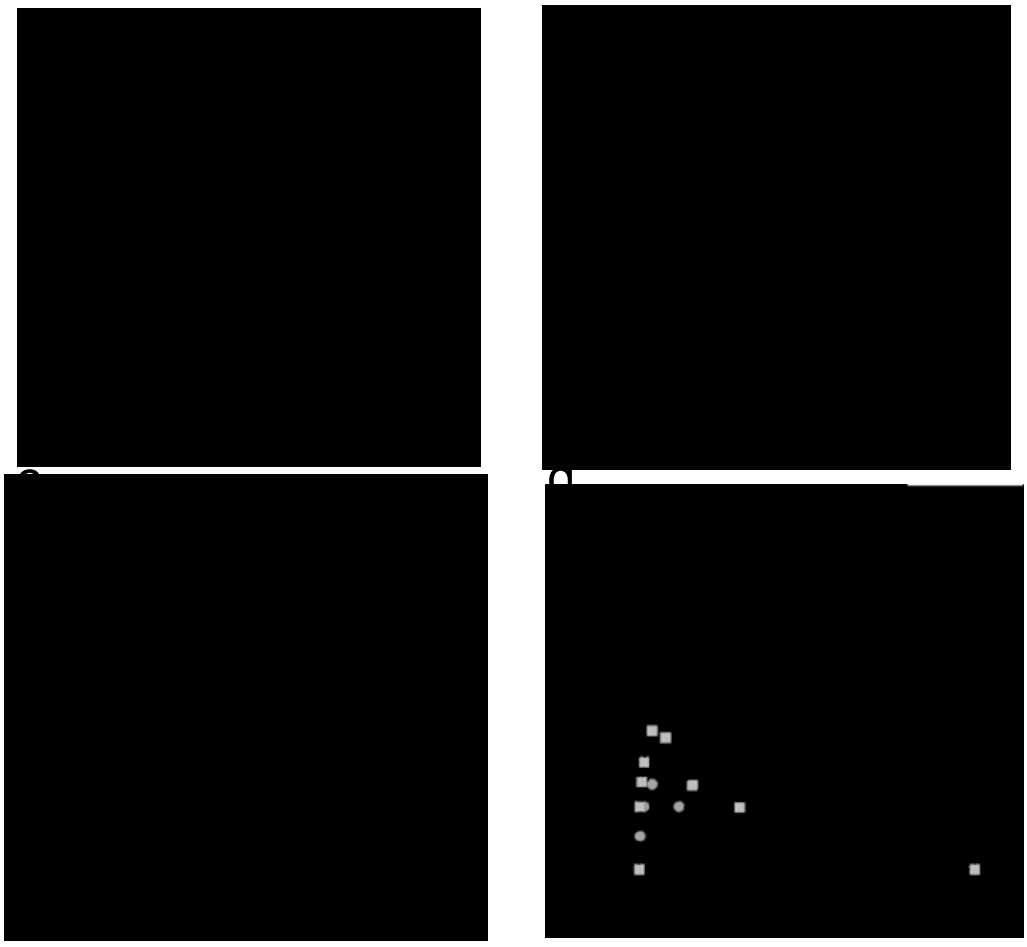

Figure 3. Rapid quench-flow analysis of ADMA turnover by DDAH. a) Acid-quenched samples at various timepoints are assayed for the presence of urea groups in reaction species EQ and Q when [ADMA] > [DDAH]; b) Acid-quenched samples at various timepoints are treated with excess base and then assayed for urea groups, representing reaction species EI, EQ, and Q when [ADMA] > [DDAH] using three different DDAH concentrations (triangles 20 μM, squares 90 μM, circles 150 μM); c) The same procedure is followed as described in b, except that [DDAH]

> [ADMA]; d) ESI-MS is used to quantify the amount of unmodified enzyme (representing E, ES and EQ species, black symbols) and enzyme bearing the *S*-alkylthiourea adduct (EI, grey symbols), using peak intensity heights of each, summed to 100% of the enzyme total, using two different concentrations of ADMA (30 μM, circles; 50 μM, squares) with 60 μM DDAH). See Materials and methods for a more complete description of reaction conditions.

2.2 Alkaline treatment of quenched samples

A second set of reaction samples were acid-quenched at various timepoints and then subsequently treated with an excess of base in order to hydrolyze the covalent *S*-alkylthiourea intermediate (E-I). Hydrolysis releases the intermediate to form additional L-citrulline product (Q) that was analyzed using the same derivatization procedure described above. Therefore, alkaline treatment of the quenched samples enables detection and quantification of the sum of three species, EQ, Q, and now in addition the *S*-alkylthiourea covalent intermediate (E-I). Conditions were chosen where ADMA concentrations exceeded that of the DDAH concentration to allow multiple turnovers. Using these procedures, we observed burst kinetics: an initial fast phase of [E-I + EQ + Q] production followed by a period of slower formation (Figure 3b). These experiments were completed using three different concentrations of enzyme, with increasing concentrations leading to larger burst amplitudes and faster linear rates in the slow phase of the reaction. The striking difference between Figures 3a and 3b is due to addition of the covalent intermediate (E-I) to the species that are quantified. A similar set of timepoints were collected and analyzed using the same procedure but using an enzyme concentration in excess of substrate concentration to approach single turnover conditions. In this experiment, a pronounced burst phase is also observed (Figure 3c). These observations are consistent with that expected for a reaction involving a covalent intermediate in which a slow step follows intermediate formation. Global fitting is described below.

2.3 ESI-MS of acid quenched samples

A third set of reaction samples were acid-quenched at various timepoints and subsequently submitted under denaturing conditions for electrospray ionization mass spectrometry (ESI-MS) to assay the protein component of the reaction mixture. This procedure detected two major protein peaks in the samples (Figure S1). The first peak (30,498 ± 10 Da) corresponds within error to the mass of the unlabeled protein (30,503 Da for His_6-DDAH missing the initial Met residue) and reflects the sum of three species in the proposed reaction, the unliganded enzyme (E), the portion of enzyme that is noncovalently bound to the ADMA substrate (ES), and the portion of enzyme that is noncovalently-bound to the L-citrulline product (EQ).[23] The second peak (30,655 ± 10 Da, +157 Da from the first peak) corresponds to the mass expected for the *S*-alkylthiourea covalent intermediate (E-I; +157 Da for addition of the $C_6H_{11}N_3O_2$ adduct).[23] Here, we make the assumption that each of these species has approximately equivalent ionization potentials so that the sum of the intensities for the two major peaks, unmodified DDAH (E + ES + EQ) and covalently modified DDAH (E-I), represent 100 % of the total enzyme used in each experiment. Using these procedures, we observed an initial increase in E-I formation, with corresponding decrease in (E + ES + EQ) species, followed by decay of the E-I species with a corresponding increase in the other species (Figure 3d). These experiments were completed using two different concentrations of ADMA, with a slight excess of enzyme in both experiments. These observations are consistent with a transient formation and decay of the proposed E-I covalent intermediate during turnover. Global fitting is described below.

2.4 Global fitting of the kinetic data

Using the program KinTek Global Kinetic Explorer,[33, 34] all of the data points shown in each panel in Figure 3, along with their associated experimental conditions (e.g. reactant concentrations), were used to perform a simultaneous global fit to the proposed minimal kinetic

mechanism for DDAH in Figure 2. To decrease the number of variables to be fitted, several of the parameters were fixed including the on-rate (k_1 estimated to be 100 $uM^{-1}s^{-1}$), an irreversible step for decay of the covalent intermediate (k_{-3} = 0 s^{-1}), and the dissociation constant for the L-citrulline product (8.4 mM, determined from product inhibition studies[27]). The resulting global fit is shown as a solid line in each panel of Figure 3, with the derived parameters listed with their fitting errors in Table 1. The largest fitting error is in k_{-1}, and the other fitted values are well constrained. Steady state parameters calculated from the fitted microscopic rate constants are compared with experimentally determined values (Table 1). The calculated K_m value was lower than the observed value, reflecting the less well constrained k_{-1} value which was not probed as thoroughly as the intermediate formation and decay rates. However, the calculated and observed k_{cat} values are identical within error, and k_{cat}/K_m values are also reasonably close (~8-fold difference). The fitted values for the rate constants and their associated errors indicate that the global data set is reasonably well fit by the proposed minimal kinetic mechanism. This is a minimal kinetic mechanism (Figure 2) and does not describe rates for every chemical step in the proposed reaction mechanism (Figure 1). However, it is determined that the rate constant for formation of the E-I intermediate is ≥10-fold greater than that for E-I decay, and the rate constant for the conversion of E-I to EQ matches the k_{cat} value. Therefore, these findings support the kinetic competence of the proposed covalent intermediate and disfavor an alternative mechanism in which covalent adduct formation could accumulate via an off-pathway event. We assign the rate-limiting step in substrate turnover to hydrolysis of the E-I intermediate.

Table 1. Kinetic parameters for the proposed DDAH kinetic mechanism

Parameter (units)	Fixed / Variable values	Global Fitting Results
k_1 ($\mu M^{-1}s^{-1}$)	100	fixed [a]
k_{-1} (s^{-1})	variable [b]	5,000 ± 1,000
k_2 (s^{-1})	variable	17 ± 2
k_{-2} (s^{-1})	variable	0.21 ± 0.03
k_3 (s^{-1})	variable	1.5 ± 0.1
k_{-3} (s^{-1})	0	fixed
$K_{d,\ L\text{-citrulline}}$ (μM)	8,400 ± 500 [c]	fixed
K_m (μM)	39 ± 9 [d]	4.6 (calc'd) [e]
k_{cat} (s^{-1})	1.3 ± 0.4 [d]	1.4 (calc'd)
k_{cat} / K_m ($M^{-1}s^{-1}$)	3.3×10^4	3×10^5 (calc'd)

[a] fixed: This parameter was fixed during fitting.
[b] variable: This parameter was left variable during fitting.
[c] This value taken from reference (*27*).
[d] This value taken from reference (*22*), determined for ADMA at pH 8.0.
[e] calc'd: This parameter was calculated from microscopic rate constants.

3. Conclusions

Previous studies supporting the existence of a covalent intermediate in the DDAH catalytic mechanism used either an altered substrate or a mutated enzyme to trap and characterize the covalent S-alkylthiourea adduct.*23, 24* Homology of DDAH to arginine deiminase, for which a covalent intermediate has been kinetically characterized,*25* supported the studies that proposed a similar covalent reaction mechanism for DDAH. However, the evidence for a covalent intermediate in DDAH did not include a kinetic analysis to show that formation and decay of this covalent adduct was on the reaction pathway and did not represent an off-pathway event. Here, we used acid quenching and differential chemical stability of the covalent adduct to quantify different reaction species and to assign a minimal kinetic mechanism to DDAH (Figure 4).

$$E + S \underset{5000\ s^{-1}}{\overset{100\ \mu M^{-1}s^{-1}}{\rightleftharpoons}} ES \underset{0.21\ s^{-1}}{\overset{17\ s^{-1}}{\rightleftharpoons}} E\text{-}I + P \xrightarrow{1.5\ s^{-1}} EQ \underset{K_d = 8.4\ mM}{\rightleftharpoons} E + Q$$

Figure 4. Proposed minimal kinetic mechanism for DDAH.

For the ADMA substrate, the rate constant for formation of the covalent intermediate is ~10-fold greater than that for formation of the product L-citrulline, leading us to conclude that the covalent adduct does represent an authentic on-pathway reaction intermediate. Although we anticipate a similar mechanism for human DDAH1 due to the high degree of structural similarity at the active site (Figure S2), the ADMA k_{cat} for human DDAH1 is ~46-fold lower than for *P. aeruginosa* DDAH, suggesting that more distant residues may impact reaction kinetics in a manner that is difficult to predict.[22, 35] The rate constants are similar to those reported for the *P. aeruginosa* homolog arginine deiminase, but this homolog has a lower ratio of rate constants for formation and decay of the intermediate (~2-fold).[25] Even more distantly related, the L-arginie:glycine amidinotransferase homologs react to make a similar *S*-alkylthiourea intermediate, yet these enzymes retain the intermediate until the second substrate glycine binds and reacts to form product and regenerate the free enzyme.[36] The kinetic mechanism of *P. aeruginosa* DDAH will provide a baseline for further studies to understand what aspects of these various active sites determine the longevity and reactivity of the shared intermediate, helping us to better understand the differing activities found within this mechanistically diverse enzyme superfamily.

The kinetic analysis of DDAH and the methods reported here for trapping and analyzing the reaction species represent an alternative to prior methods that use radiolabeled substrate.[25] Both the results and the methods are relevant to other studies. For example, kinetic mechanism and reaction conditions are important considerations when designing high-throughput inhibitor screening campaigns.[37] If DDAH is screened using saturating amounts of substrate, our work predicts that the majority of the enzyme will be present as the covalent E-I complex, which may unduly limit the types of inhibitors discovered. In contrast, screens that use more balanced conditions where E-I does not predominate would better enable inhibitor access to the active-site. Also, a similar acid-trapping method could possibly be applied to other members of the enzyme superfamily to trap reaction intermediates, or in the case of protein arginine deiminases, to trap

and identify protein substrates. Apart from its previous use in characterizing covalent inhibitor adducts, the differential pH stability of covalent adducts was successfully used here for trapping and quantifying reaction intermediates and also has wider potential applications.

4. Materials and methods

4.1 Protein expression and purification

Heterologous overexpression and purification of wild-type *N*-terminal His_6-tagged DDAH from *P. aerug*inosa was completed as previously described, except that the induced cultures were grown overnight before harvesting to minimize nonenzymatic *N*-terminal gluconylation.[23] Protein concentration was determined using UV-vis spectroscopy and a calculated ε_{280} (17,210 $M^{-1}cm^{-1}$) after denaturation in guanidine HCl (6M), as described previously.[23]

4.2 Rapid quench-flow, general procedure

A RQF-3 rapid quench-flow apparatus (KinTek, Snow Shoe, PA) was used to collect reaction timepoints, all determined at 25 °C, and all were acid quenched using 0.6 M trifluoroacetic acid (TFA) and a constant quench volume option (88 μL). The instrument was calibrated according to the manufacturer's protocols, including volume quantification of the individual reaction loops and calibration of motor speed. Each reaction, initiated by the computer-controlled step motor, resulted in quenched timepoints between 0.005 and 5 s depending on the experiment and were collected in 1.5 mL microcentrifuge tubes for later analysis. Representative samples were measured to determine they consistently had a pH value ≤ 1. Tests for enzyme activity after the quench revealed no measurable residual activity (not shown).

4.3 Analysis for the reaction species EQ and Q

The substrate ADMA in Reaction Buffer (200 mM Tris, 100 mM KCl, 0.5 mM EDTA, pH 7.5) was mixed with purified *P. aeruginosa* DDAH in the same buffer using the RQF-3 instrument with the final reaction concentrations estimated to be 20% of syringe concentrations according to control runs and instrument calibrations (ADMA 2 mM, DDAH 90 μM). Timepoints between 0.005

– 0.8 s were collected. The concentration of urea functional groups contained in each quenched sample (e.g. L-citrulline) was quantified using a derivatization procedure described previously as the COLDER assay to produce a colored product that can be quantified by UV-vis spectroscopy.[31, 32] A calibration curve was prepared using L-citrulline standards (0 – 313 μM). Pre-quenched DDAH samples were also run to enable subtraction of background absorbance. Freshly prepared COLDER reagent (1 mL) was added to all samples, the tubes were sealed, placed in a boiling water bath for 15 min, cooled for 10 min at 25 °C, and then the absorbance of each at 540.5 nm was measured using a Cary 50 UV-vis spectrophotometer (Varian Inc, Walnut Creek, CA), with experimental samples quantified by reference to the standard curve. Please note that appropriate caution and safeguards should be used when heating these sealed microcentrifuge tubes due to the risk of the tube breeching and violent release of the concentrated acids within.

4.4 Analysis for the reaction species EI, EQ, and Q

Rapid quench timepoints were collected as described above in section 4.3 using three different final reaction conditions (20 μM DDAH, 2 mM ADMA; 90 μM DDAH, 2 mM ADMA; 150 μM DDAH, 2.2 mM ADMA). To convert any trapped *S*-alkylthiourea adduct with DDAH into additional L-citrulline, each of the quenched samples were treated with 80 μL of the strong base KOH (10 M). The pH of representative samples was determined to be ≥ 14 and no residual enzyme activity was detected (not shown). These samples were subsequently quantified for urea groups using the COLDER reagent as described above. An additional experiment using these same procedures was also completed under conditions where final reaction concentrations of the enzyme DDAH (50 μM) exceeded that of the substrate ADMA (8 μM) to approximate single turnover conditions.

4.5 ESI-MS analysis of quenched samples

Rapid quenched timepoints between 0.01 – 5 s were collected as described above in section 4.3 using two different final reaction conditions (60 μM DDAH, 30 μM ADMA; 60 μM DDAH, 50 μM ADMA). Samples were submitted to the Analytical Instrumentation Facility Core (College of Pharmacy, University of Texas, Austin) and were analyzed by electrospray ionization mass spectrometry (ESI-MS) using a ThermoFinnigan LCQ ion trap mass spectrometer (ThermoFinnigan, San Jose, CA) equipped with a Michrom Magic 2002 HPLC system as described previously.[23, 38] Spectra were acquired continuously in the centroid mode over the mass range of *m/z* 350 – 2000. The deconvoluted masses were calculated using ThermoFinnigan's Xcalibur 1.3 Bio-Works 3.0 software with approximately 40 spectra averaged. Peak intensity heights corresponding to unmodified enzyme and enzyme containing the *S*-alkylthiourea covalent adduct[23] were added to approximate 100% of the enzyme used in each run, and each species plotted as a percentage of this total.

4.6 Global fitting to a minimal kinetic mechanism

Experimental values and reaction conditions were entered into the global fitting program KinTek Global Kinetic Explorer version 8.0.190104 (KinTek, Snow Shoe, PA).[33, 34] Using the constraints described in the above text and summarized in Table 1, a global fit was determined to all of the experiments simultaneously, with the fitting errors reported. Fits were exported and replotted using KaleidaGraph version 4.5 (Synergy Software, Reading, PA).

Acknowledgements

On occasion of this virtual special issue honoring Richard Silverman, we thank Dr. Silverman (Northwestern University, Evanston, IL) for his mentorship, his numerous contributions to bioorganic and medicinal chemistry and his training of generations of medicinal chemists. We

thank Ken Johnson (University of Texas, Austin) for the generous gift of the KinTek Explorer software package. We thank Kevin Dalby (University of Texas, Austin) for use of the rapid quench-flow instrument.

Funding: This work was supported in part by the National Science Foundation (Grant CHE-1904514 to W.F.) and the Robert A. Welch Foundation (Grant F-1572 to W.F.).

Appendix A. Supplementary material

Supplementary data to this article can be found online at …

References

1. Cinelli, M. A., Do, H. T., Miley, G. P., and Silverman, R. B. (2020) Inducible nitric oxide synthase: Regulation, structure, and inhibition, *Med Res Rev 40*, 158-189.
2. Cary, S. P., Winger, J. A., Derbyshire, E. R., and Marletta, M. A. (2006) Nitric oxide signaling: no longer simply on or off, *Trends Biochem Sci 31*, 231-239.
3. Mukherjee, P., Cinelli, M. A., Kang, S., and Silverman, R. B. (2014) Development of nitric oxide synthase inhibitors for neurodegeneration and neuropathic pain, *Chem Soc Rev 43*, 6814-6838.
4. Saha, B. K., and Burns, S. L. (2020) The Story of Nitric Oxide, Sepsis and Methylene Blue: A Comprehensive Pathophysiologic Review, *Am J Med Sci 360*, 329-337.
5. Burke, A. J., Sullivan, F. J., Giles, F. J., and Glynn, S. A. (2013) The yin and yang of nitric oxide in cancer progression, *Carcinogenesis 34*, 503-512.
6. Huang, H., Hah, J. M., and Silverman, R. B. (2001) Mechanism of nitric oxide synthase. Evidence that direct hydrogen atom abstraction from the O-H bond of N^G-hydroxyarginine is not relevant to the mechanism, *J Am Chem Soc 123*, 2674-2676.
7. Fast, W., Nikolic, D., VanBreemen, R. B., and Silverman, R. B. (1999) Mechanistic studies of the inactivation of inducible nitric oxide synthase by N^5-(1-iminoethyl)-L-ornithine (L-NIO), *J Am Chem Soc 121*, 903-916.
8. Cinelli, M. A., Reidl, C. T., Li, H., Chreifi, G., Poulos, T. L., and Silverman, R. B. (2020) First Contact: 7-Phenyl-2-Aminoquinolines, Potent and Selective Neuronal Nitric Oxide Synthase Inhibitors That Target an Isoform-Specific Aspartate, *J Med Chem 63*, 4528-4554.
9. Do, H. T., Li, H., Chreifi, G., Poulos, T. L., and Silverman, R. B. (2019) Optimization of Blood-Brain Barrier Permeability with Potent and Selective Human Neuronal Nitric Oxide Synthase Inhibitors Having a 2-Aminopyridine Scaffold, *J Med Chem 62*, 2690-2707.
10. Zhu, Y., Nikolic, D., Van Breemen, R. B., and Silverman, R. B. (2005) Mechanism of inactivation of inducible nitric oxide synthase by amidines. Irreversible enzyme inactivation without inactivator modification, *J Am Chem Soc 127*, 858-868.
11. Leiper, J., and Nandi, M. (2011) The therapeutic potential of targeting endogenous inhibitors of nitric oxide synthesis, *Nat Rev Drug Discov 10*, 277-291.
12. Shirakawa, T., Kako, K., Shimada, T., Nagashima, Y., Nakamura, A., Ishida, J., and Fukamizu, A. (2011) Production of free methylarginines via the proteasome and autophagy pathways in cultured cells, *Mol Med Rep 4*, 615-620.
13. Cardounel, A. J., and Zweier, J. L. (2002) Endogenous methylarginines regulate neuronal nitric-oxide synthase and prevent excitotoxic injury, *J Biol Chem 277*, 33995-34002.
14. Silverman, R. B. (1995) Mechanism-based enzyme inactivators, *Methods Enzymol 249*, 240-283.
15. Tuley, A., and Fast, W. (2018) The Taxonomy of Covalent Inhibitors, *Biochemistry 57*, 3326-3337.
16. Olken, N. M., and Marletta, M. A. (1993) N^G-methyl-L-arginine functions as an alternate substrate and mechanism-based inhibitor of nitric oxide synthase, *Biochemistry 32*, 9677-9685.
17. Ogawa, T., Kimoto, M., and Sasaoka, K. (1989) Purification and properties of a new enzyme, N^G,N^G-dimethylarginine dimethylaminohydrolase, from rat kidney, *J Biol Chem 264*, 10205-10209.
18. Leiper, J., Nandi, M., Torondel, B., Murray-Rust, J., Malaki, M., O'Hara, B., Rossiter, S., Anthony, S., Madhani, M., Selwood, D., Smith, C., Wojciak-Stothard, B., Rudiger, A., Stidwill, R., McDonald, N. Q., and Vallance, P. (2007) Disruption of methylarginine metabolism impairs vascular homeostasis, *Nat Med 13*, 198-203.
19. Zolner, J., Lambden, S., Nasri, N. M., Johnson, M. R., and Leiper, J. (2020) Inhibition of Dimethylarginine Dimethylaminohydrolase 1 Improves the Outcome of Sepsis in Pregnant Mice, *Shock 54*, 498-506.

20. Hulin, J. A., Tommasi, S., Elliot, D., and Mangoni, A. A. (2019) Small molecule inhibition of DDAH1 significantly attenuates triple negative breast cancer cell vasculogenic mimicry in vitro, *Biomed Pharmacother 111*, 602-612.
21. Linsky, T. W., and Fast, W. (2010) Guanidine-Modifying Enzymes in the Pentein Superfamily, In *Comprehensive Natural Products Chemistry II, Chemistry and Biology* (Mander, L., and Liu, H.-w., Eds.), pp 125-159, Elsevier, Oxford.
22. Stone, E. M., Costello, A. L., Tierney, D. L., and Fast, W. (2006) Substrate-assisted cysteine deprotonation in the mechanism of dimethylargininase (DDAH) from *Pseudomonas aeruginosa*, *Biochemistry 45*, 5618-5630.
23. Stone, E. M., Person, M. D., Costello, N. J., and Fast, W. (2005) Characterization of a transient covalent adduct formed during dimethylarginine dimethylaminohydrolase catalysis, *Biochemistry 44*, 7069-7078.
24. Linsky, T. W., Monzingo, A. F., Stone, E. M., Robertus, J. D., and Fast, W. (2008) Promiscuous partitioning of a covalent intermediate common in the pentein superfamily, *Chem Biol 15*, 467-475.
25. Lu, X., Galkin, A., Herzberg, O., and Dunaway-Mariano, D. (2004) Arginine deiminase uses an active-site cysteine in nucleophilic catalysis of L-arginine hydrolysis, *J Am Chem Soc 126*, 5374-5375.
26. Smith, D. W., and Fahrney, D. E. (1978) Catalysis by arginine deiminase: evidence for a covalent intermediate, *Biochem Biophys Res Commun 83*, 101-106.
27. Stone, E. M., and Fast, W. (2005) A continuous spectrophotometric assay for dimethylarginine dimethylaminohydrolase, *Anal Biochem 343*, 335-337.
28. Murray-Rust, J., Leiper, J., McAlister, M., Phelan, J., Tilley, S., Santa Maria, J., Vallance, P., and McDonald, N. (2001) Structural insights into the hydrolysis of cellular nitric oxide synthase inhibitors by dimethylarginine dimethylaminohydrolase, *Nat Struct Biol 8*, 679-683.
29. Silverman, R. B., Hiebert, C. K., and Vazquez, M. L. (1985) Inactivation of monoamine oxidase by allylamine does not result in flavin attachment, *J Biol Chem 260*, 14648-14652.
30. Olson, G. T., Fu, M., Lau, S., Rinehart, K. L., and Silverman, R. B. (1998) An aromatization mechanism for inactivation of gamma-aminobutyric acid aminotransferase for the antibiotic L-cycloserine, *J Am Chem Soc 120*, 2256-2267.
31. Knipp, M., and Vasak, M. (2000) A colorimetric 96-well microtiter plate assay for the determination of enzymatically formed citrulline, *Anal Biochem 286*, 257-264.
32. Johnson, C. M., Linsky, T. W., Yoon, D. W., Person, M. D., and Fast, W. (2011) Discovery of halopyridines as quiescent affinity labels: inactivation of dimethylarginine dimethylaminohydrolase, *J Am Chem Soc 133*, 1553-1562.
33. Johnson, K. A. (2009) Fitting enzyme kinetic data with KinTek Global Kinetic Explorer, *Methods Enzymol 467*, 601-626.
34. Johnson, K. A., Simpson, Z. B., and Blom, T. (2009) Global kinetic explorer: a new computer program for dynamic simulation and fitting of kinetic data, *Anal Biochem 387*, 20-29.
35. Hong, L., and Fast, W. (2007) Inhibition of human dimethylarginine dimethylaminohydrolase-1 by *S*-nitroso-L-homocysteine and hydrogen peroxide. Analysis, quantification, and implications for hyperhomocysteinemia, *J Biol Chem 282*, 34684-34692.
36. Humm, A., Fritsche, E., and Steinbacher, S. (1997) Structure and reaction mechanism of L-arginine:glycine amidinotransferase, *Biol Chem 378*, 193-197.
37. Holdgate, G. A., Meek, T. D., and Grimley, R. L. (2018) Mechanistic enzymology in drug discovery: a fresh perspective, *Nat Rev Drug Discov 17*, 78.
38. Wang, S. C., Person, M. D., Johnson, W. H., Jr., and Whitman, C. P. (2003) Reactions of trans-3-chloroacrylic acid dehalogenase with acetylene substrates: consequences of and evidence for a hydration reaction, *Biochemistry 42*, 8762-8773.

Supplementary material for

On the kinetic mechanism of dimethylarginine dimethylaminohydrolase (DDAH)

*Corey M. Johnson and Walter Fast **

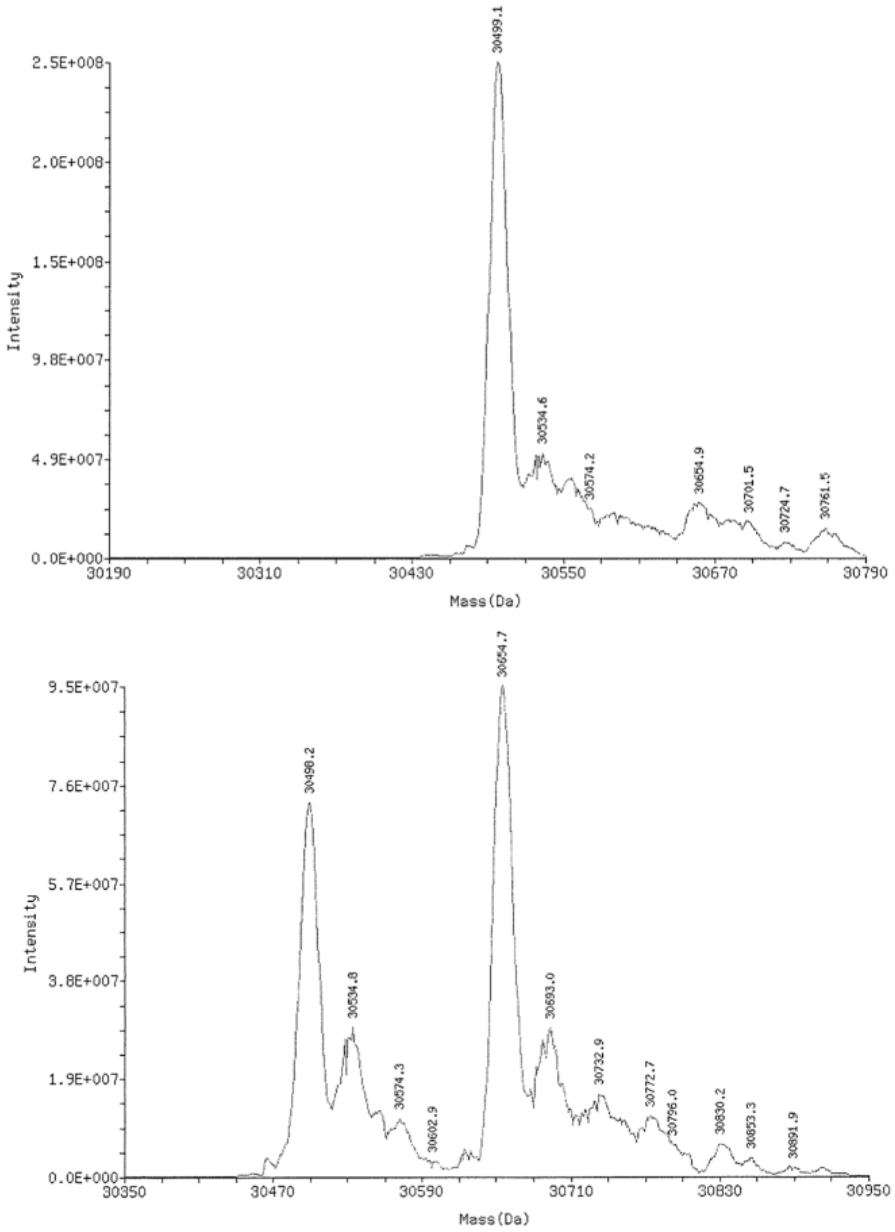

Figure S1. Example ESI-MS spectrums for quenched samples. Top: Control sample in which DDAH (90 μM) is prequenched with TFA and then mixed with ADMA (2 mM) before ESI-MS analysis. The peak with the highest intensity is at 30,499 ± 10 Da, corresponding to the unmodified enzyme (see main text). Bottom: Experimental sample where DDAH (90 μM) is mixed with ADMA (2 mM) and acid quenched after 0.01 s, followed by ESI-MS to reveal the two peaks with the highest intensities at 30,498 and 30,655 ± 10 Da, corresponding to the unmodified enzyme and the enzyme bearing the *S*-alkylthiourea adduct.

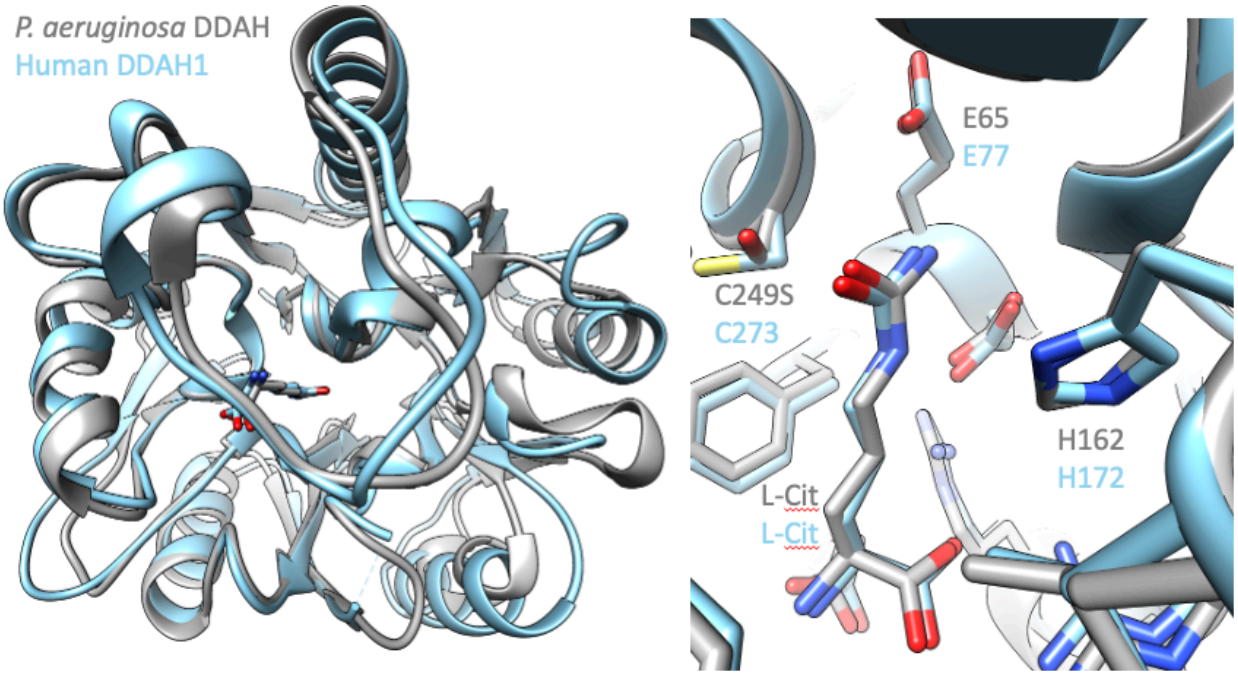

Figure S2. Overlay of product-bound structures of two DDAH orthologs. Left) The overall structure of *P. aeruginosa* DDAH (grey) and human DDAH-1 (light blue) are superimposed and show very similar overall folds using a ribbon view to depict the path of the backbones. Right) The active-site residues and L-citrulline binding orientation are superimposed from the *P. aeruginosa* (grey) and human DDAH1 (light blue) structures. The *P. aeruginosa* DDAH has an active-site C294S mutation. All of the residues in close proximity to the L-citrulline product, excepting the C294S mutation are found in very similar orientations between the human and *P. aeruginosa* orthologs. The structures are derived from protein data bank accession codes 1h70 and 2jai and are superimposed using UCSF Chimera. (J. Murray-Rust et al **2001** *Nat Struct Biol 8*, 679-683; J. Leiper et al **2007** *Nat Med 13*, 198-203; E.F. Pettersen et al **2004** *J Comput Chem 25*, 1605-1612.)